Japanese Journal of Applied Physics
Vol. 46, No. 8B, 2007, pp. 5626–5630

©2007 The Japan Society of Applied Physics

Kelvin Probe Force Microscopy without Bias-Voltage Feedback

Osamu TAKEUCHI*, Yoshihisa OHRAI, Shoji YOSHIDA, and Hidemi SHIGEKAWA

Institute of Applied Physics, CREST-JST, 21st Century COE, University of Tsukuba, Tsukuba, Ibaraki 305-8573, Japan

(Received January 30, 2007; revised May 16, 2007; accepted May 19, 2007; published online August 23, 2007)

A variation of Kelvin probe force microscopy that does not require bias-voltage feedback for contact potential difference (CPD) detection was proposed. Two independent lock-in amplifiers were used to measure the first- and second-order derivatives of the electrostatic force exerted on the cantilever, and CPD was deductively determined from these signals. The application of this technique to the unsaturated Au/Si(111)-5 × 2 system confirmed that the instability of the measurement system resulting from bias-voltage feedback can be completely eliminated and that CPD measurement at a finite bias voltage is possible. [DOI: 10.1143/JJAP.46.5626]

KEYWORDS: Kelvin probe force microscopy, atomic force microscopy

1. Introduction

Kelvin probe force microscopy (KFM)[1,2] is known as one of the most powerful measurement techniques for visualizing the nanometer-scale variation of a sample surface's electrostatic potential that is possibly modulated by localized charges and dipole moments at the surface. KFM has been applied to a variety of metal, semiconductor and organic surfaces to study, for example, the photochemical reactions on surfaces, next-generation data storage devices and primitive electronic devices.[3–8] KFM is based on the measurement of the contact potential difference (CPD) between the apex of the conductive cantilever probe of a noncontact atomic force microscopy (nc-AFM) system and the local sample surface area under the probe. Since CPD is defined as the surface potential difference between two objects, the CPD variation observed in KFM directly reflects the spatial variation in the surface potential of the sample surface relative to that of the probe apex. In conventional KFM, CPD is obtained using a bias-voltage-feedback circuit that nullifies the electric field between the probe and the sample. Thus, it fundamentally involves instability of measurement system due to the possible oscillation of the feedback loop. The instability must be prevented by having the feedback gain low; then, however, the measurement takes quite a long time. In order to eliminate the instability fundamentally, in this study, we investigated a new setup for KFM that does not involve bias-voltage feedback and clarified its advantages and disadvantages with respect to the conventional method.

2. KFM without Bias-Voltage Feedback

At first, we will review the fundamentals of KFM. When the conductive cantilever probe approaches the sample surface, it experiences the interaction force F induced by the sample surface. Generally, F is composed of the atomic force $F_{\rm atom}$ and the electrostatic force $F_{\rm es}$. The former is the sum of the van der Waals force and chemical bonding force, and the latter reflects CPD:

$$F = F_{\rm atom} + F_{\rm es}. \tag{1}$$

The electrostatic component originates from the charge that is stored in the capacitance C formed between the probe and the sample surface. The component can be expressed as the derivative of the electrostatic energy $E_{\rm es}$ stored in the capacitance with respect to the probe–sample distance z:

$$F_{\rm es} = \frac{dE_{\rm es}}{dz} = \frac{1}{2}\frac{dC}{dz}(V_{\rm CPD} - V_{\rm s})^2. \tag{2}$$

Here, $V_{\rm CPD}$ is the contact potential difference and $V_{\rm s}$ is the sample bias voltage. The frequency shift Δf measured in nc-AFM is approximately proportional to the derivative of the interaction force with respect to z:

$$\Delta f \propto \frac{dF}{dz} = \frac{dF_{\rm atom}}{dz} + \frac{1}{2}\frac{d^2C}{dz^2}(V_{\rm CPD} - V_{\rm s})^2. \tag{3}$$

Here, it is assumed that $V_{\rm CPD}$ is not a function of z. Note that this condition might not occur on an insulating surface or a semiconductor surface with a low density of surface state due to the leakage of the electric field into the sample.[9,10] Equation (3) indicates that the total frequency shift as a function of $V_{\rm s}$ is a parabolic function, which has the minimum at $V_{\rm s} = V_{\rm CPD}$, as illustrated in Fig. 1(a).

In a conventional KFM, the first derivative of $\Delta f(V_{\rm s})$ is detected by a lock-in amplifier with sample-bias-voltage modulation, as illustrated in Fig. 2(a). The obtained $\Delta f'(V_{\rm s})$ is proportional to the difference between $V_{\rm s}$ and $V_{\rm CPD}$, as illustrated in Fig. 1(b):

$$\Delta f'(V_{\rm s}) \propto \frac{d^2C}{dz^2}(V_{\rm s} - V_{\rm CPD}). \tag{4}$$

Negatively feeding back this value to the bias voltage with an appropriate gain results in the automatic adjustment of $V_{\rm s}$ to $V_{\rm CPD}$. Thus, recording the bias voltage, with the probe scanned over the sample surface, enables the mapping of CPD. Typical experimental conditions are a bias modulation frequency of 1 kHz, a bias modulation amplitude of 1 V and a scan rate of 20 min/image. KFM often takes quite a long time because one cannot have too large gain for the bias-voltage-feedback circuit to prevent the instability of the measurement system owing to the oscillation of the feedback circuit.

Here, we propose a new technique to determine CPD without a bias-voltage-feedback circuit. Instead, another lock-in amplifier is added to the system to measure the second harmonic component of the frequency shift, as illustrated in Fig. 3. This signal gives the second-order derivative of the frequency shift $\Delta f''(V_{\rm s})$. Since the first derivative is a linear function, this value is constant against the bias voltage, as illustrated in Fig. 1(c).

*E-mail address: takeuchi@bk.tsukuba.ac.jp

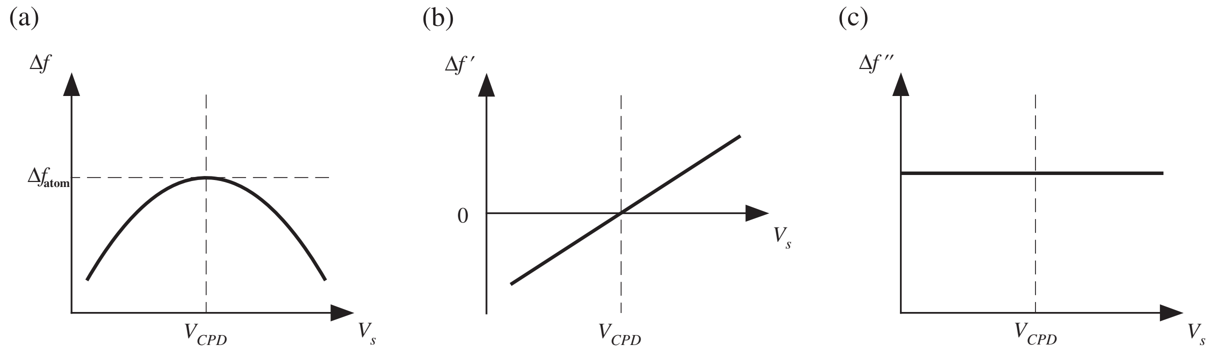

Fig. 1. Bias voltage dependences of (a) primitive, (b) first-, and (c) second-order derivatives of frequency shift in nc-AFM.

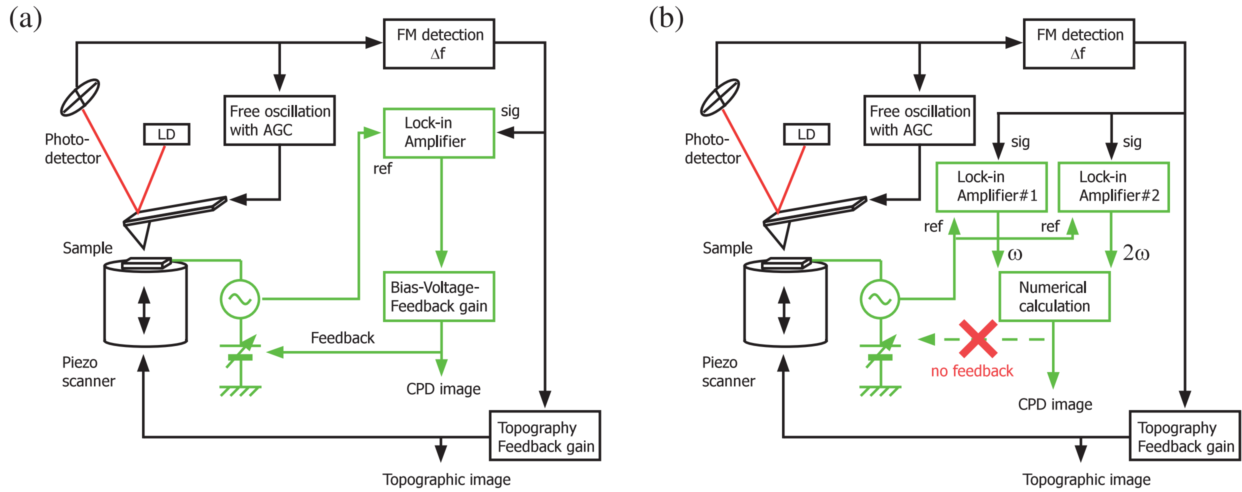

Fig. 2. Schematics of KFM systems: (a) conventional system with bias-voltage feedback, (b) proposed system without bias-voltage feedback.

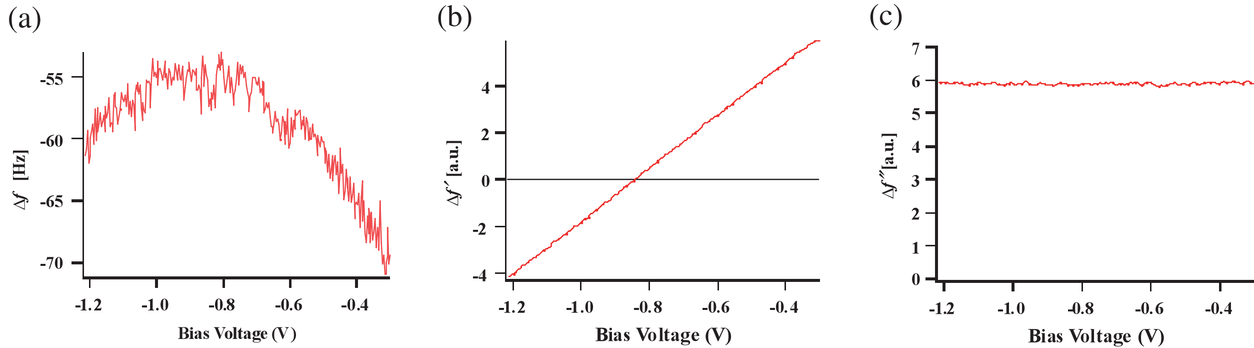

Fig. 3. Experimental bias voltage dependences of (a) frequency shift, (b) ω-component from lock-in amplifier, and (c) 2ω-component from lock-in amplifier.

$$\Delta f''(V_s) \propto \frac{d^2C}{dz^2} = \text{const.} \tag{5}$$

Thus, if $\Delta f'$ and $\Delta f''$ are measured simultaneously at a certain bias voltage, V_s^0, V_{CPD} can be derived as

$$V_{CPD} = V_s^0 - \Delta f'(V_s^0)/\Delta f''(V_s^0). \tag{6}$$

Since this method does not involve the bias-voltage feedback, it is free from the instability due to such feedback. In the next section, we demonstrate the characteristics of this technique using a well-known heteroepitaxy system of an unsaturated Au/Si(111)-5 × 2 surface.

3. Experimental Procedure

The experiment was performed with a commercial ultrahigh vacuum nc-AFM system (Omicron VT-STM/AFM) whose base pressure was less than 1×10^{-8} Pa. The Si substrate, mounted on a sample holder, was degassed for ~10 h before being flash heated to ~1200 °C to remove the oxide layer. Then, the substrate was slowly cooled in order to form a well-ordered Si(111)-7 × 7 structure. Gold deposition was performed using a tungsten filament at a rate of ~1 ML/min at a substrate temperature of 650 °C. The measurement was carried out at room temperature using a

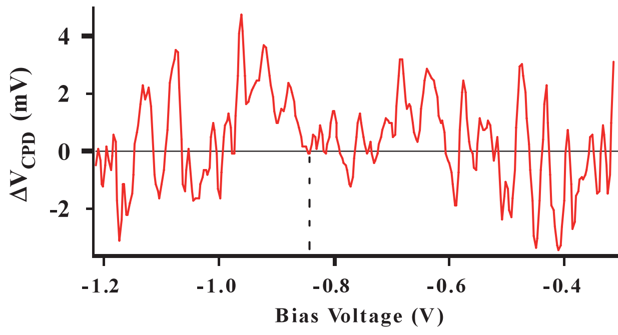

Fig. 4. Calculated CPD from experimental results in Fig. 3. The precision of the measurement was determined to be 2–3 mV.

Ti–Pt-coated cantilever with a spring constant of 5.0 N/m and a resonant frequency of 160 kHz (MikroMasch). The amplitude and frequency of the bias-voltage modulation were 1 V_{rms} and 1020 Hz, respectively. Unless otherwise stated, the time constant for the two lock-in amplifiers (Stanford Research Systems SR830) was 10 ms with a slope of -6 dB/oct. Outputs from the lock-in amplifiers were connected to the auxiliary inputs of the AFM electronics to be stored. Then, the CPD image was numerically calculated off-line using data analysis software (WaveMetrics Igor Pro).

4. Results and Discussion

At first, $\Delta f(V_s)$, $\Delta f'(V_s)$, and $\Delta f''(V_s)$ curves were measured for a Si(111)-7 × 7 surface to verify the validity of the above discussion. For the curve measurements, the probe–sample separation was determined with a sample bias voltage of $V_s = -1.2$ V, a sample bias modulation of 1 V_{rms}, and a reference frequency shift of -61 Hz. Once these conditions were achieved, the probe position was fixed with the z-piezo feedback disabled. Then, bias voltage was swept from -1.2 to 0.5 V in 4.1 s. The result is shown in Fig. 3. As seen, the curves are well described by the theoretical prediction shown in Fig. 1. Sometimes, however, slight deviations were observed owing to the small variation in probe–sample distance during the curve measurement (data not shown). Since such variations are due to the thermal drift of the system or the creep of the z-piezo device, once a stable condition is achieved, no reproducible deviation was noticeable.

To examine the detection accuracy of the new procedure, the CPD was calculated using eq. (6) and all the measured points in the curves in Figs. 3(b) and 3(c). The result is plotted in Fig. 4 as the deviation from the zero-cross voltage of the $\Delta f'(V_s)$ curve. Even though Δf exhibits relatively large noise in this experiment, CPD was determined with a precision of 2–3 mV, confirming the effectiveness of the proposed technique. This precision can, of course, be improved by using a larger time constant for lock-in detection or, more desirably, by increasing the reference frequency shift. Since increasing the reference frequency shift increases $\Delta f''$, the effect of detection error in $\Delta f'$ and $\Delta f''$ is reduced in eq. (6).

One point must be considered for the analysis. Although the Δf measurement bandwidth of the current state-of-the-art nc-AFM systems is sufficiently high for modulation measurements at a frequency of ~1 kHz, a small phase shift and the attenuation of the signal owing to the finite bandwidth is unavoidable. Thus, the calibration of the signal is necessary to compensate for this effect. We define the lock-in outputs for ω and 2ω components as X_ω and $X_{2\omega}$. These signals are related to $\Delta f'$ and $\Delta f''$ as

$$X_\omega = A\Delta f'(V_s)\Delta V_s, \quad X_{2\omega} = B\Delta f''(V_s)\Delta V_s^2/2, \tag{7}$$

where ΔV_s is the modulation amplitude and A and B are measurement-system-dependent coefficients that are slightly smaller than unity. Note that A and B also differ from each other because the signal frequencies are different. To determine CPD using eq. (6), eq. (7) can be rewritten as

$$\frac{\Delta f'(V_s)}{\Delta f''(V_s)} = \left(\frac{B}{A}\right)\frac{\Delta V_s(X_\omega/X_{2\omega})}{2} \tag{8}$$

Thus, we need to determine the ratio B/A, which is dependent on the detector bandwidth of Δf and the modulation frequency. This ratio can be obtained by measuring a set of $X_\omega(V_s)$ and $X_{2\omega}(V_s)$ curves at one place on the sample as follows. The average slope of $X_\omega(V_s)$ gives

$$\langle dX_\omega/dV_s\rangle = A\langle\Delta f''\rangle\Delta V_s, \tag{9}$$

and the average of $X_{2\omega}(V_s)$ gives

$$\langle X_{2\omega}\rangle = B\langle\Delta f''\rangle\Delta V_s^2/2. \tag{10}$$

Here, the brackets denote the average over the measured voltage range. Thus, the ratio can be calculated as

$$\frac{B}{A} = 2\left\langle\frac{dX_\omega}{dV_s}\right\rangle^{-1}\frac{\langle X_{2\omega}\rangle}{\Delta V_s}. \tag{11}$$

In our experimental setup, this ratio was about 10% smaller than unity, reflecting a slightly larger attenuation for the 2ω component. As long as metallic sample surfaces are measured, this ratio is independent of the physical system being measured; it is only dependent on the bandwidth of the measurement system and the fundamental modulation frequency. Thus, calibration is required only one time for a series of measurements. Finally, CPD can be obtained from $X_\omega(V_s^0)$ and $X_{2\omega}(V_s^0)$ as

$$V_{CPD} = V_s^0 - \left\langle\frac{dX_\omega}{dV_s}\right\rangle^{-1}\langle X_{2\omega}\rangle\left[\frac{X_\omega(V_s^0)}{X_{2\omega}(V_s^0)}\right]. \tag{12}$$

Next, the spatial variation of CPD was confirmed with a partially covered Au/Si(111)-5 × 2 system. Figure 5 shows the results. The measurement conditions were $V_s = 0.2$ V and $\Delta f_{ref} = -60$ Hz. As can be seen, the Au-covered areas on the sample were imaged as clear depressions in the topography and $\Delta f'$ images, and as convexes in the $\Delta f''$ and CPD images. The measured difference in CPD between the Au-covered and uncovered parts was always consistent with those of previous reports.[8] On the other hand, the contrasts in the topography, $\Delta f'$ and $\Delta f''$ images were highly dependent on bias voltage. The images in Fig. 6 were measured using the same sample with the same probe but with a different bias voltage $V_s = 1.2$ V. In this case, neither the topography nor $\Delta f''$ images showed noticeable contrast ($\Delta f''$ image not shown). This is because the observed height difference in the topography was almost completely due to the F_{es} component of eq. (1). The structural corrugation of

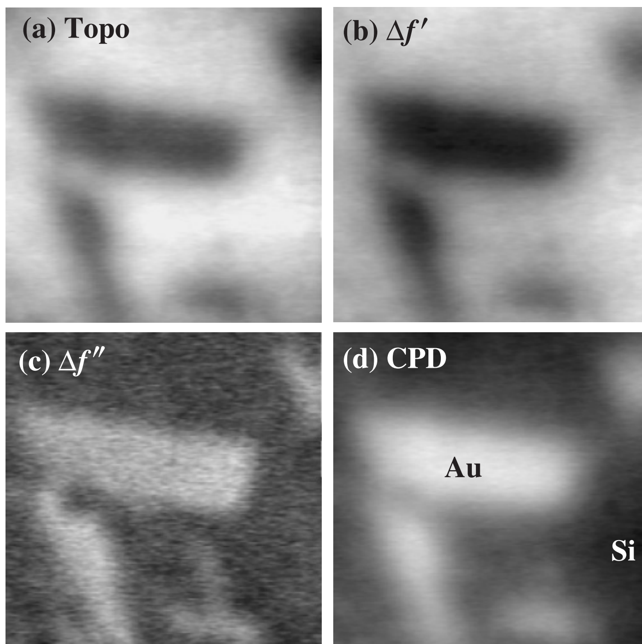

Fig. 5. Images of unsaturated Au/Si(111)-5 × 2 surface taken using new method: (a) topography, (b) ω-component from lock-in amplifier, (c) 2ω-component from lock-in amplifier, and (d) CPD, at $V_s = 0.2$ V, scan rate of 17 min/image, scan size of $300 \times 300\,\text{nm}^2$, and 256 scan lines.

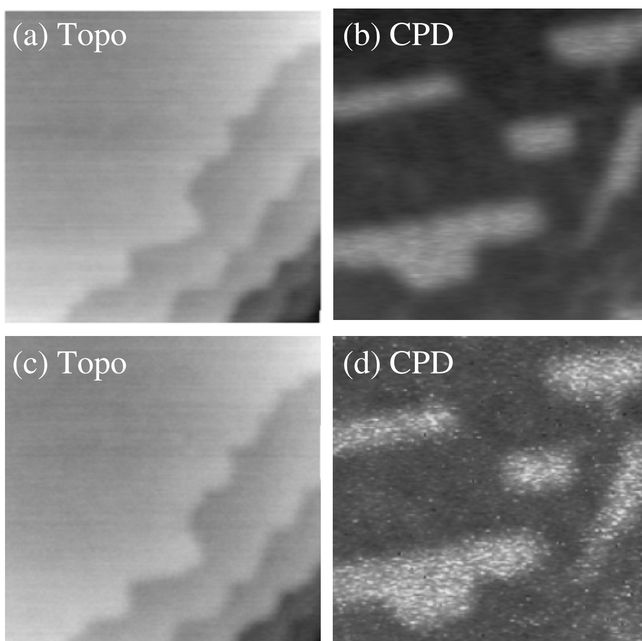

Fig. 6. Images taken using new method at different scan rates: (a), (b) topography and CPD images taken with scan rate of 13 min/image and lock-in time constant of 10 ms; and (c), (d) images taken with scan rate of 3 min/image and lock-in time constant of 1 ms. For both cases, the other conditions were $V_s = 1.2$ V, a scan size of $450 \times 450\,\text{nm}^2$ and 256 scan lines.

the surface was negligible. In such cases, when the sample bias voltage is applied at the mid point between the CPD's of the Au-covered and uncovered domains, the probe feels exactly same F_{es} in different domains, although the polarity of the electric field in different domains is reversed. In addition, since $\Delta f''$ is directly dependent on probe–sample separation, $\Delta f''$ also appears flat.

Strong electrostatic force can be observed when a finite electric field exists between the probe and the sample. This is also important in terms of the spatial resolution and the sensitivity of measurement. When the sample bias voltage is markedly different from CPD, the probe feels a large electrostatic force. Thus, the z-piezo feedback circuit separates the probe from the surface to maintain the frequency shift at the reference value. This causes the spatial resolution of the topography and CPD images to become poor. Furthermore, when the probe–sample separation becomes large, $\Delta f'$ becomes large and $\Delta f''$ becomes small. As a result, a small error in $\Delta f'$ and $\Delta f''$ detection largely affect the determination of CPD using eq. (6). Consequently, for a precise measurement, the sample bias voltage should be as close to the average CPD in the imaging area as possible. Note that this condition is also preferred in a normal nc-AFM measurement.

The images in Fig. 6 were taken at the bias voltage optimized as described above. Note that the spatial resolutions are improved compared with those in Fig. 5. Now, we will discuss the scanning speed and noise level in KFM. Figures 6(a) and 6(b) show topography and CPD images simultaneously taken at a rate of 13 min/image with a lock-in time constant of 10 ms, and Figs. 6(c) and 6(d) show topography and CPD images taken at a rate of 3 min/image with a time constant of 1 ms. When scan rate is increased, a broader signal detection bandwidth is required to measure the more quickly changing signals. From this point of view, at first glance, the new KFM system seems superior to the conventional system, because when the same time constant is used for the lock-in amplifiers, the signal from the new system responds four to ten times more quickly than that from the conventional system. This is because, in the conventional system, the signal is further delayed owing to the feedback circuit.

However, taking the signal-to-noise ratio into account, the conclusion becomes different. When the signal bandwidth is further limited by the bias-voltage-feedback circuit in the conventional system, the noise power is also reduced by this limited bandwidth. Thus, if a signal-to-noise ratio on the same order is required in the new system, the lock-in time constant must be selected to be longer. In other words, unless the noise power in Δf is extremely small, the effective measurement bandwidth is not limited by the experimental setup but rather by the required signal-to-noise ratio. Consequently, the advantage of the new system is not that it directly provides an improved scan rate. Instead, it is that it provides an instability-free way of optimizing the scan rate in order to achieve the required signal-to-noise ratio. As shown in Figs. 6(c) and 6(d), the new system is completely stable even when the signal-to-noise ratio in the CPD image is quite low. In such a case, the conventional system easily becomes unstable and rams the probe into the sample surface.

Another advantage of the new system is its ability to image surface potential under a finite bias voltage. On semiconductor and insulator surfaces, it is known that the surface potential is often bias voltage dependent.[9–11] The details of the dependence contains useful information on material properties, such as the dielectric constant, the dopant density and the carrier density. For such an

application, however, the primary limitation is that, when the surface potential changes with respect to bias voltage modulation for KFM, the correct values for $\Delta f'$ and $\Delta f''$ cannot be obtained. The experimental conditions must be carefully chosen to overcome this problem.

5. Conclusions

In summary, a new measurement technique for KFM was proposed and its validity was confirmed by its application to the unsaturated Au/Si(111)-5×2 system. The new technique replaces the bias-voltage-feedback circuit of the conventional KFM system with a second lock-in amplifier. As a result, the instability of the bias-voltage-feedback loop was completely eliminated. Since the new method can measure the contact potential difference under a finite bias voltage between the probe and the sample, its future application to semiconductor or insulating samples is suggested.

Acknowledgement

This work was supported in part by a Grant-in-Aid for Scientific Research from the Ministry of Education, Culture, Sports, Science, and Technology of Japan.

1) J. M. R. Weaver and D. W. Abraham: J. Vac. Sci. Technol. B **9** (1991) 1559.
2) M. Nonnenmacher, M. P. O'Boyle, and H. K. Wickramasinghe: Appl. Phys. Lett. **58** (1991) 2921.
3) B. Rezek and C. E. Nebel: Diamond Relat. Mater. **14** (2005) 466.
4) Y. Miyato, K. Kobayashi, K. Matsushige, and H. Yamada: Jpn. J. Appl. Phys. **44** (2005) 1633.
5) J. Y. Son, B. G. Kim, C. H. Kim, and J. H. Cho: Appl. Phys. Lett. **84** (2004) 4971.
6) M. Ishii and B. Hamilton: Appl. Phys. Lett. **85** (2004) 1610.
7) T. F. Xie, K. Kumada, S. Kishimoto, and T. Mizutani: Jpn. J. Appl. Phys. **42** (2003) 1751.
8) S. Kitamura and M. Iwatsuki: Appl. Phys. Lett. **72** (1998) 3154.
9) S. Yoshida, J. Kikuchi, Y. Kanitani, O. Takeuchi, H. Oigawa, and H. Shigekawa: e-J. Surf. Sci. Nanotechnol. **4** (2006) 192.
10) X. Q. Chen, H. Yamada, T. Horiuchi, K. Matsushige, S. Watanabe, M. Kawai, and P. S. Weiss: J. Vac. Sci. Technol. B **17** (1999) 1930.
11) S. Yoshida, Y. Kanitani, R. Oshima, Y. Okada, O. Takeuchi, and H. Shigekawa: Phys. Rev. Lett. **98** (2007) 026802.